Induction machine transfer functions and dynamic response by means of complex time variables

IEEE Transactions on Power Apparatus and Systems, Vol. PAS-95, no. 4, July/August 1976

INDUCTION MACHINE TRANSFER FUNCTIONS AND DYNAMIC RESPONSE BY MEANS OF COMPLEX TIME VARIABLES

D. W. Novotny
University of Wisconsin - Madison

J. H. Wouterse
Eindhoven Technical University

ABSTRACT

The symmetry of the induction machine can be exploited to obtain general closed form expressions for the small signal transfer functions describing speed, voltage, frequency, or load perturbations by utilizing the complex time variables introduced by Ku and Lyon in the 1950's.

After a brief introduction to complex variables, the linearized complex variable equations describing small signal dynamic performance are presented. These equations are used to obtain transfer functions in which the effects of excitation level are isolated in the gain factors. The speed and frequency dependence of the poles and zeros is expressed in closed form employing a useful non-dimensional parameter system.

To illustrate the application of these results, the dynamic behavior of the induction machine without feedback control is analyzed. It is shown that the general dynamic response can be characterized by the non-dimensional loop gain and stator frequency. A set of general non-dimensional root loci are presented which permit rapid estimation of the relative stability (dominant eigenvalues) and the frequency of minimum damping of any specific machine. The application of the transfer functions to cases involving feedback control of the machine is also discussed.

INTRODUCTION

Unlike a dc machine, the dynamic response of an induction machine is of high order and no generally applicable simple model exists to predict performance and assist in design.[1] Computer simulations,[2-6] linearized models requiring numerical evaluation of eigenvalues or transfer functions,[7-10] and simple approximate models[10-12] have been employed with varying degrees of success. Of these methods, the numerical calculation of transfer characteristics[9] has the advantage of avoiding direct simulation and yet not being subject to the limitations inherent in the approximate methods. This approach, however, has the disadvantage of being entirely numerical and thus not capable of producing general results without extensive computation.

The basic difficulty in any analytical approach is the high order and non-linearity of even the idealized model of an ac machine. Linearization methods are useful, but the resulting linear models are of high order and involve the operating point constraints in a very complicated manner. The only obvious possibility of simplifying these descriptions and obtaining general closed form results lies in the structural symmetry of the induction machine. The successful and routine utilization of this symmetry in steady state analysis is a good example of the immense simplification which is attainable by this means.

Paper F 76 196-6, recommended and approved by the IEEE Rotating Machinery Committee of the IEEE Power Engineering Society for presentation at the IEEE PES Winter Meeting & Tesla Symposium, New York, N.Y., January 25-30, 1976. Manuscript submitted August 29, 1975; made available for printing November 21, 1975.

In a search for a method to exploit the symmetry, the complex variable analysis introduced by Ku[13] and Lyon[14] and extensively employed outside of the U.S.[15-17] appeared to hold promise. Except for isolated instances[18,19] this method has been ignored in favor of real variable analysis in the U.S.

The results of employing complex variables to de-couple and otherwise simplify the mathematical description of induction machine dynamics are presented in this paper. This initial report incorporates voltage, frequency and speed feedback but excludes cases utilizing current feedback. The analysis is also restricted to linear symmetric source impedances. Subsequent work to include current feedback and inverter dc side source impedance is under way. An analysis of inverter performance[20] and steady state performance of an inverter fed induction machine[21] using complex variables have been completed.

COMPLEX TIME DOMAIN MODEL

The machine model employed in the study is the conventional idealized machine with power invariant two phase variables.[22] The development presented in Appendix A first transforms the three phase machine to a two phase power invariant equivalent and subsequently combines the two phase variables into complex variables such that the symmetry of the real variable equations is made evident. Except for the constants associated with power invariency, the results are the same as Lyon's original work.[14]

With the notation defined in Appendix A, the induction machine is represented in a synchronous reference by the two complex variable equations

$$\begin{aligned} \bar{v}_{s\omega} &= \bar{Z}_{s\omega}\,\bar{i}_{s\omega} + \bar{Z}_{m\omega}\,\bar{i}_{r\omega} \\ 0 &= \bar{Z}_{d\omega}\,\bar{i}_{s\omega} + \bar{Z}_{r\omega}\,\bar{i}_{r\omega} \end{aligned} \tag{1}$$

in which the impedances as given in (A-16) are complex operational impedances containing the derivative operator p and the instantaneous frequencies ω and ω_s (stator and slip frequency respectively). The instantaneous torque equation is

$$T = nM\ \mathrm{Im}[\bar{i}_{s\omega}\,\bar{i}^{*}_{r\omega}] = (J/n)p\omega_r + T_L \tag{2}$$

These complex variable equations are exactly equivalent to the 4×4 matrix equation and the torque equation used in real variable theory (see (A-3) and (A-4)). For balanced polyphase excitation Appendix A yields the complex variable applied voltage as

$$\bar{v}_{s\omega} = \sqrt{3}\,V_{rms}\,\varepsilon^{j(\phi-\phi_g)} \tag{3}$$

and it is convenient but not essential to choose $\phi = \phi_g$ such that $\bar{v}_{s\omega}$ is a real quantity.

In addition to the obvious advantages of simplicity and compactness, a major advantage of the complex variable equations is the reduction of the order of the voltage equations from four to two. Clearly the order has been reduced by means of the special symmetry associated with the machine; the system is still fourth order but complex variables decouple the fourth order system into two second order systems which are complex conjugates. Only one of the second order systems need be solved since the solution to the second is simply the complex conjugate of the first solution. The situation is

similar to the decoupling which takes place in steady state analysis where only one phase need be solved with the solutions for the other phases being obtained by introducing the appropriate phase shift.

SMALL SIGNAL COMPLEX VARIABLE EQUATIONS

As given in (1) to (3) the complex variable equations are non-linear in the same way as the real variable equations. A linearization can be carried out as for real variables by allowing small variations in the voltages, currents, frequencies, speed and torque. The details are given in Appendix B; the results are

$$\Delta\bar{v}_s = \bar{Z}_s\Delta\bar{i}_s + \bar{Z}_m\Delta\bar{i}_r + \bar{\phi}_{so}\Delta\omega$$
$$0 = \bar{Z}_d\Delta\bar{i}_s + \bar{Z}_r\Delta\bar{i}_r + \bar{\phi}_{ro}(\Delta\omega - \Delta\omega_r) \quad (4)$$

$$\Delta T = nM\,\mathrm{Im}[\bar{i}_{so}\,\Delta\bar{i}_r^* + \Delta\bar{i}_s\,\bar{i}_{ro}^*] = \frac{J}{n}\,p\Delta\omega_r + \Delta T_L \quad (5)$$

where the Δ-variables are the small signal quantities, subscript o-variables are steady state quantities, and the complex operational impedances now involve only steady state frequencies as shown in (B-7). In addition to these small signal equations, the steady state equations defining the operating point are also available as given in (B-3). The steady state impedances are, of course, not operational impedances but simply complex numbers which depend on the speed and frequency of the operating point.

Simplification of Small Signal Equations

To this point, except for the reduction in order, the complex variable equations are simply a compact version of the real variable equations; nothing beyond a saving of space has really been accomplished. However, the simplicity of the equations now permits a series of simplifications and changes in form which would be difficult with real variables.

The steady state rotor voltage equation (B-3) yields a very simple relation between the steady state currents

$$\bar{i}_{so} = -(\bar{Z}_{ro}/\bar{Z}_{do})\bar{i}_{ro} \quad (6)$$

which can be used to eliminate the steady state stator current from (4) and (5). Using this result the steady state fluxes become

$$\bar{\phi}_{so} = -\frac{L_s}{M}\frac{\bar{Z}'_{ro}}{\omega_{so}}\bar{i}_{ro} \qquad \bar{\phi}_{ro} = -\frac{R_r}{\omega_{so}}\bar{i}_{ro} \quad (7)$$

where $\bar{Z}'_{ro}$ is $\bar{Z}'_{ro} = R_r + j\omega_{so}\sigma L_r$. The torque equation (5) can also be rewritten using (6) in a much more convenient form involving only $\bar{I}_{ro}$ and ω_{so} (after some manipulation). With these changes the small signal equations become

$$\Delta\bar{v}_s + \left(\frac{L_s}{M}\frac{\bar{Z}'_{ro}}{\omega_{so}}\bar{i}_{ro}\right)\Delta\omega = \bar{Z}_s\,\Delta\bar{i}_s + \bar{Z}_m\Delta\bar{i}_r$$
$$\frac{R_r}{\omega_{so}}\,i_{ro}(\Delta\omega - \Delta\omega_r) = \bar{Z}_d\,\Delta\bar{i}_s + \bar{Z}_r\,\Delta\bar{i}_r \quad (8)$$

$$\Delta T = \frac{n}{\omega_{so}}\,\mathrm{Re}[\bar{i}^*_{ro}(\bar{Z}^*_{do}\,\Delta\bar{i}_s + \bar{Z}^*_{ro}\,\Delta\bar{i}_r)] = \frac{J}{n}p\Delta\omega_r + \Delta T_L \quad (9)$$

in which only the steady state rotor current occurs, along with the steady state stator and slip frequency, to define the operating point. From a conceptual point of view (8) and (9) suggest the block diagram shown in Fig. 1a. The nature of the transfer properties of this diagram is the subject of the remainder of the paper.

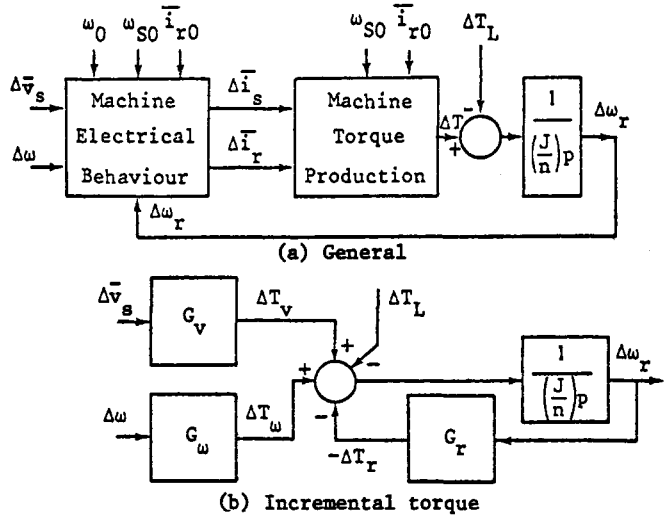

Fig. 1. Block diagram representation of the induction machine.

OPEN LOOP TRANSFER FUNCTIONS

If the feedback path in Fig. 1a is opened, the various transfer functions of the diagram can be obtained by simple complex variable algebra. With these open loop transfer functions available, subsequent analysis to evaluate the effect of the internal feedback loop (speed voltages) or externally applied feedback paths can be carried out using any of the various methods of linear feedback analysis.

Incremental Currents

Considering the incremental voltage, frequency, and rotor speed as independent variables, (8) can be solved for the incremental currents to yield

$$\Delta\bar{i}_s = \frac{1}{\bar{Z}^2}\left[\bar{Z}_r\Delta\bar{v}_s + \frac{\bar{I}_{ro}}{\omega_{so}}R_r\bar{Z}_m\,\Delta\omega_r + \frac{\bar{I}_{ro}}{\omega_{so}}\left(\frac{L_s}{M}\bar{Z}'_{ro}\,\bar{Z}_r - R_r\bar{Z}_m\right)\Delta\omega\right]$$
$$\Delta\bar{i}_r = \frac{1}{\bar{Z}^2}\left[-\bar{Z}_d\Delta\bar{v}_s - \frac{\bar{I}_{ro}}{\omega_{so}}R_r\bar{Z}_s\,\Delta\omega_r - \frac{\bar{I}_{ro}}{\omega_{so}}\left(\frac{L_s}{M}\bar{Z}'_{ro}\,\bar{Z}_d - R_r\bar{Z}_s\right)\Delta\omega\right] \quad (10)$$

where $\bar{Z}^2 = \bar{Z}_s\bar{Z}_r - \bar{Z}_m\bar{Z}_d$. In effect, (10), defines a set of six transfer functions relating the incremental currents to the incremental input variables $\Delta\bar{v}_s$, $\Delta\omega_r$, $\Delta\omega$. Each of these six complex variable transfer functions can be utilized to obtain several real variable transfer functions (describing magnitude, phase, in phase component, etc.). These current transfer functions will not be developed further in this paper in order that attention can be centered on the more immediately applicable incremental torque functions.

Incremental Torque Transfer Functions

The incremental torque can now be evaluated by substituting the incremental currents (10) into the torque equation (9). It is convenient to immediately define torque transfer functions and treat each independent variable separately. This is illustrated in Fig. 1b where the three incremental torque transfer functions for $\Delta\bar{v}_s$, $\Delta\omega$, and $\Delta\omega_r$ are applied to express the properties of Fig. 1a in conventional block diagram form. For convenience, the feedback transfer function G_r is defined to include a minus sign to allow drawing the diagram with the normal negative feedback convention.

With the conventions and symbols established in Fig. 1b, the speed feedback transfer function becomes

$$G_r = -\frac{\Delta T_r}{\Delta\omega_r} = -\frac{\Delta T}{\Delta\omega_r}\bigg|_{\Delta\bar{v}_s,\Delta\omega=0} \tag{11}$$

which can be evaluated using (9) and (10)

$$G_r = \frac{n}{\omega_{so}} \mathrm{Re}\left[\bar{i}^*_{ro}\left(\bar{z}^*_{ro}\frac{\bar{i}_{ro}}{\omega_{so}}\frac{R_r\bar{z}_s}{\bar{z}^2} - \bar{z}^*_{do}\frac{\bar{i}_{ro}}{\omega_{so}}\frac{R_r\bar{z}_m}{\bar{z}^2}\right)\right] \tag{12}$$

Rationalizing the complex expression by multiplying by $(\bar{z}^2)^*$ and using the result $\bar{i}_{ro}\bar{i}^*_{ro} = |\bar{i}_{ro}|^2$ yields

$$G_r = \frac{n|\bar{i}_{ro}|^2 R_r}{\omega^2_{so}} \frac{\mathrm{Re}[(\bar{z}^*_{ro}\bar{z}_s - \bar{z}^*_{do}\bar{z}_m)(\bar{z}^2)^*]}{|\bar{z}^2|^2} \tag{13}$$

This result is remarkable in several respects:

1) the real multiplier (gain) is immediately recognizable as the steady state torque divided by slip frequency T_o/ω_{so},
2) the demoninator $|\bar{z}^2|^2$ (poles of the transfer function) is a fourth order polynomial in p which is automatically factored into $\bar{z}^2(\bar{z}^2)^*$, the product of a complex quadratic and its conjugate,[14,15,16,18]
3) the numerator complex expression which depends only on machine parameters, speed, and frequency, represents a closed form expression for the zeros.

The simplification and decoupling which has been accomplished by applying complex variables is extremely valuable. The dependence of the resulting transfer function on the steady state operating point has been greatly simplified; only T_o and ω_{so} appear in the gain and only ω_o and ω_{so} in the poles and zeros. The problem of finding the poles is reduced from a fourth order to a quadratic problem and a closed form expression for the zeros has been obtained.

Similar operations yield the other incremental torque transfer functions defined as

$$G_\omega = \frac{\Delta T_\omega}{\Delta\omega} = \frac{\Delta T}{\Delta\omega}\bigg|_{\Delta\omega_r,\Delta\bar{v}_s=0} \tag{14}$$

$$G_v = \frac{\Delta T_v}{\Delta v_s} = \frac{\Delta T}{\Delta v_s}\bigg|_{\Delta\omega_r,\Delta\omega=0} \tag{15}$$

In each case the poles are given by the same expression involving $\bar{z}^2$. The gain and complex expressions for the zeros are summarized in Table I. In (15) $\Delta\bar{v}_s$ is treated as a real quantity (see (3)) and the transfer function represents the torque change resulting from a change in voltage magnitude. A transfer function for voltage phase changes can also be found if needed. To obtain the results in Table I for G_v, the relation between $\bar{I}_{ro}$ and $\bar{v}_{so}$ given by the stator equation in (B-3) is needed to allow extraction of the steady state voltage from inside the Re operator. Note that the gain factor in G_v contains an additional term compared to G_ω and G_r.

Evaluation of Poles and Zeros

The remaining task is to evaluate the complex expressions in the transfer functions to obtain the poles and zeros. The nature of this problem can be illustrated by examining the complex valued quadratic defining the poles of (13).

$$\bar{z}^2 = \bar{z}_s\bar{z}_r - \bar{z}_m\bar{z}_d = 0 \tag{16}$$

Carrying out the multiplication of the complex operational impedances results in

$$0 = \sigma L_s L_r p^2 + (R_s L_r + R_r L_s)p + R_s R_r - \sigma L_s L_r \omega_o(\omega_o - \omega_{ro}) + j[\sigma L_s L_r(2\omega_o - \omega_{ro})p + (R_s L_r + R_r L_s)\omega_o - R_s L_r \omega_{ro}] \tag{17}$$

The complex roots of this equation in p are the poles (eigenvalues) of the transfer functions. The complete set of four poles is obtained by complementing these roots by their conjugates. A somewhat more complicated expression which is a real valued cubic equation in p results from expanding the numerator line of (13).

NORMALIZED OPEN LOOP TRANSFER FUNCTIONS

To produce results in a form convenient for general use it is helpful to introduce a normalized time variable and to replace the conventional machine impedances with a set of non-dimensional parameters. The normalized system is based on the machine time constants and places the relative importance of the machine parameters regarding dynamic performance in better perspective.

Non-Dimensional Variables

The base of the normalized variables is chosen as the rotor transient decrement factor (reciprocal of transient time constant). The non-dimensional variables are:

$\alpha = \frac{\alpha_s}{\alpha_r} = \frac{T'_r}{T'_s} \approx \frac{R_s}{R_r}$ ratio of transient decrement factors

$\sigma = 1 - M^2/L_sL_r$ leakage parameter

$\tilde{\omega} = \omega/\alpha_r$ normalized frequency

$\lambda = p/\alpha_r$ normalized eigenvalue

where

$\alpha_r = R_r/\sigma L_r = 1/T'_r$ rotor transient decrement factor

$\alpha_s = R_s/\sigma L_s = 1/T'_s$ stator transient decrement factor

This normalization results in much simpler expressions for the poles and zeros and expresses all decrements and frequencies as multiples of the rotor transient decrement factor α_r.

Normalized Transfer Functions

In terms of normalized variables the transfer functions are expressed in the form

$$\tilde{G}_x = \tilde{K}_x \frac{\tilde{N}_x}{\tilde{D}} \tag{18}$$

where $\tilde{N}_x$ and $\tilde{D}$ are dimensionless expressions for the zeros and poles respectively. For convenience, the coefficient of the highest power of λ is always reduced to unity. The gain factor K_x carries the dimensions of the particular transfer function under study.

Non-Dimensional Constant Speed Eigenvalues (Poles)

The non-dimensional form of (16) and (17) are

$$\bar{z}^2 = \sigma L_s L_r \alpha_r^2 \tilde{D} = 0 \tag{19}$$

$$\tilde{D} = \lambda^2 + (1+\alpha)\lambda + \sigma\alpha - \tilde{\omega}_o\tilde{\omega}_{so} + j((\tilde{\omega}_o + \tilde{\omega}_{so})\lambda + \alpha\tilde{\omega}_{so} + \tilde{\omega}_o) \tag{20}$$

from which the solutions to $\bar{z}^2 = 0$ can be expressed as

$$\lambda = -j\tilde{\omega}_{so} - \tfrac{1}{2}\left[1+\alpha + j\tilde{\omega}_{ro} \pm \sqrt{(1+\alpha)^2 - 4\sigma\alpha - \tilde{\omega}_{ro}^2 + j2(\alpha-1)\tilde{\omega}_{ro}}\right] \tag{21}$$

Table I. Summary of transfer functions

Transfer function	Complex expression	Normalized gain $\tilde{K}_x$	Non-dimensional polynomial for zeros $\tilde{N}_x$
$G_r = -\frac{\Delta T}{\Delta\omega_r}$	Gain = T_o/ω_{so}	$\tilde{K}_r = \frac{T_o}{\omega_{so}}$	$\lambda^3 \times 1$
$\Delta\bar{v}_s = 0$	Zeros = $\mathrm{Re}[(\bar{Z}^*_{ro}\bar{Z}_s - \bar{Z}^*_{do}\bar{Z}_m)(\bar{Z}^2)^*]$		$\lambda^2 \times 1+\alpha+\sigma\alpha-\tilde{\omega}^2_{so}$
$\Delta\omega = 0$			$\lambda^1 \times \tilde{\omega}^2_o + 2\sigma\alpha + \sigma\alpha^2 - 2\alpha\tilde{\omega}^2_{so}$
			$\lambda^o \times \tilde{\omega}^2_o+\sigma^2\alpha^2-\tilde{\omega}^2_{so}(\alpha^2+\tilde{\omega}^2_o)$
$G_\omega = \frac{\Delta T}{\Delta\omega}$	Gain = T_o/ω_{so}	$\tilde{K}_\omega = \frac{T_o}{\omega_{so}}\left(\frac{1}{A}\right)$	$\lambda^2 \times 1$
$\Delta\bar{v}_s = 0$			$\lambda^1 \times A(\tilde{\omega}^2_o+\sigma\alpha(1+\alpha)-\tilde{\omega}_{so}(2\tilde{\omega}_o+\alpha\tilde{\omega}_{so}))$
$\Delta\omega_r = 0$	Zeros = $\mathrm{Re}\left[\left((\bar{Z}^*_{ro}\bar{Z}_s - \bar{Z}^*_{do}\bar{Z}_m) - (L_s/R_rM)\bar{Z}'_{ro}(\bar{Z}^*_{ro}\bar{Z}_d - \bar{Z}^*_{do}\bar{Z}_r)\right)(\bar{Z}^2)^*\right]$	$A = 1/(\sigma\alpha - \tilde{\omega}_o\tilde{\omega}_{so})$	$\lambda^o \times A(\tilde{\omega}^2_o+\sigma^2\alpha^2-2\tilde{\omega}_o\tilde{\omega}_{so} - \tilde{\omega}^2_{so}(\tilde{\omega}^2_o+\alpha(2+\alpha-2\sigma)+2\tilde{\omega}_o\tilde{\omega}_{so}))$
$G_v = \frac{\Delta T}{\Delta v_s}$	Gain = $\frac{n V_{so}}{\omega_{so}}$	$\tilde{K}_v = \frac{T_o}{\omega_{so}}\frac{\alpha_r}{V_{so}}\left(\frac{1}{B}\right)$	$\lambda^3 \times 1$
$\Delta\omega_r = 0$	Zeros = $\mathrm{Re}\left[\frac{(\bar{Z}_{ro}\bar{Z}^*_d - \bar{Z}_{do}\bar{Z}^*_r)\bar{Z}_{do}(\bar{Z}^2)}{\bar{Z}_{so}\bar{Z}_{ro} - \bar{Z}_{mo}\bar{Z}_{do}}\right]$	$B = 1/(\alpha\tilde{\omega}_{so}+\tilde{\omega}_o)$	$\lambda^2 \times 1+\alpha+B(\tilde{\omega}_o-\tilde{\omega}_{so})(\tilde{\omega}_o\tilde{\omega}_{so}-\sigma\alpha)$
$\Delta\omega = 0$			$\lambda^1 \times 2B\tilde{\omega}_{so}(\tilde{\omega}^2_o+\sigma\alpha(1+\alpha)+\alpha\tilde{\omega}^2_{so})$
			$\lambda^o \times 2\tilde{\omega}_{so}(B(\tilde{\omega}_o\tilde{\omega}_{so}-\sigma\alpha)^2+1/B)$

This closed form expression for the eigenvalues has the useful property that the normalized slip frequency $\tilde{\omega}_{so}$ enters as a simple linear term and thus affects only the frequency and not the decrement. Therefore, a single solution for a given rotor speed is sufficient for all values of slip; it is only necessary to subtract $\tilde{\omega}_{so}$ from the j-part of the zero slip eigenvalue to obtain the actual eigenvalue.

Figure 2, which for convenience is drawn for the conjugate of (21) in order to show the positive j-axis, is a representative set of eigenvalues for $\sigma = 0.05$. The figure actually gives the eigenvalues in a rotor reference; the speed of the reference system affects only the j-part of the eigenvalues. Adding the slip frequency $\tilde{\omega}_{so}$ to the j-part converts to a synchronous reference as explained above.

Note that the eigenvalue variation for higher speeds (Fig. 2a) is quite simple. An excellent approximation for $\tilde{\omega}_{ro} > 3$ and α near unity is

$$\lambda = -\alpha \pm j\left(\tilde{\omega}_{ro} - \frac{(\alpha+1)^2}{4\tilde{\omega}_{ro}} + \tilde{\omega}_{so}\right), \quad -1 \pm j\left(\frac{(\alpha+1)^2}{4\tilde{\omega}_{ro}} + \tilde{\omega}_{so}\right) \qquad (22)$$

Thus for these higher speeds one eigenvalue has a frequency slightly greater than slip frequency and a decrement equal to the rotor decrement and the other is near stator frequency and has a decrement equal to the stator decrement.

For lower speeds (Fig. 2b) the variation of the eigenvalues becomes more complicated. The wide separation in frequency characteristic of higher speeds gradually disappears and is replaced by a wide separation in decrements which reaches a maximum at zero speed. Note that the $\alpha = 1$ curve is unique in that a double complex eigenvalue occurs for a speed slightly below 2.0. For other values of α the two branches are always separate. In this low speed region the value of σ also becomes important and Fig. 2b should only be used to indicate trends, the correct eigenvalues must be found from (21).

Non-Dimensional Zeros

The complex variable expressions for the zeros of the transfer functions make the determination of the polynomials defining the zeros a straightforward operation. However, the resulting polynomials are often cubic and the zeros must be located by approximation or by numerical methods. The non-dimensional polynomial and the corresponding gain factor for each of the three torque transfer functions defined previously is given in Table I. A major advantage of these polynomials expressing the zeros is their use in obtaining approximate zero locations and in estimating the effects of parameter or operating point changes. This type of application is illustrated later in the paper.

OVERALL TRANSFER FUNCTIONS WITH FINITE INERTIA

The transfer function relating a change in one of the input variables to a change in speed or torque is obtained by using Fig. 1b in combination with the results summarized in Table I. Because the open loop transfer functions all have the same poles, there are simple relations between the overall functions and the open loop functions.

Speed Transfer Functions

As an example, the overall relation between a change in frequency and a change in speed is (in normalized form)

$$\left.\frac{\Delta\tilde{\omega}_r}{\Delta\tilde{\omega}}\right|_{\Delta\bar{v}_s=0} = \tilde{G}_\omega \frac{(n/J\alpha_r\lambda)}{1+\tilde{G}_r(n/J\alpha_r\lambda)} \qquad (23)$$

Multiplying through by the common denominator $\tilde{D}$ of $\tilde{G}_\omega$ and $\tilde{G}_r$ yields

$$\left.\frac{\Delta\tilde{\omega}_r}{\Delta\tilde{\omega}}\right|_{\Delta\bar{v}_s=0} = \left(\frac{n\tilde{K}_\omega}{J\alpha_r}\right)\frac{\tilde{N}_\omega}{\tilde{D}\lambda + (n\tilde{K}_r/J\alpha_r)\tilde{N}_r} \qquad (24)$$

which demonstrates the following facts:

1) the overall gain is $n/J\alpha_r$ times the gain of $\tilde{G}_\omega$
2) the overall zeros are the zeros of $\tilde{G}_\omega$
3) the poles of the overall function are the roots of the characteristic equation $D\lambda + (n\tilde{K}_r/J\alpha_r)\tilde{N}_r = 0$.

The gain and zeros for voltage or load torque as the input quantity can be obtained in the same manner. The poles of all the transfer functions are the same and are given by the characteristic equation associated with (23) or (24).

Torque Transfer Functions

If the output quantity of interest is the machine torque it is only necessary to multiply the corresponding speed function by the reciprocal of the inertia function $J\alpha_r\lambda/n$. This has the effect of multiplying the overall gain factor by $J\alpha_r/n$ and modifies the zeros by adding a zero at the origin. The poles are unchanged.

Transfer Functions for Constant Slip

As an example of external feedback control, consider a speed loop arranged to hold constant slip by varying the applied frequency. Such a loop would place $\tilde{G}_\omega$ in parallel with G_r to produce a new function $\tilde{G}_s$

$$\tilde{G}_s = \tilde{G}_r - \tilde{G}_\omega = -\frac{\Delta T}{\Delta\omega_r}\bigg|_{\Delta\bar{v}_s,\Delta\tilde{\omega}_s=0} \tag{25}$$

With $\tilde{G}_s$ available (by combining results from Table I) the overall transfer functions can be obtained as in the previous sections. Note that this external feedback loop would result in new system poles but would not affect the gain factors or zeros.

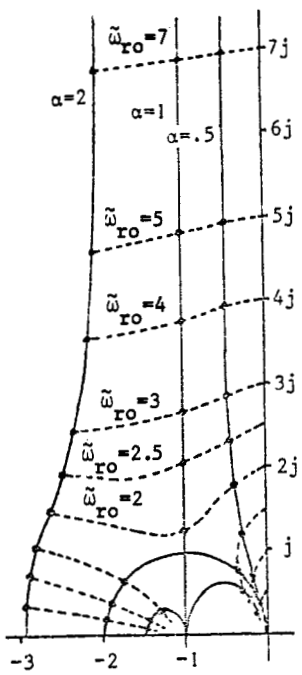

Fig. 2a. High speed eigenvalues.

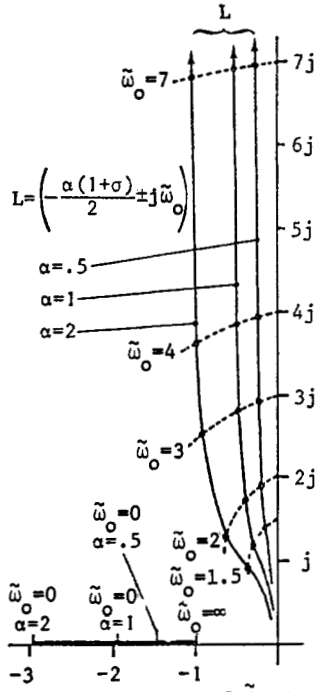

Fig. 3. Zeros of $\tilde{G}_r$ for no load and $\sigma = 0.05$.

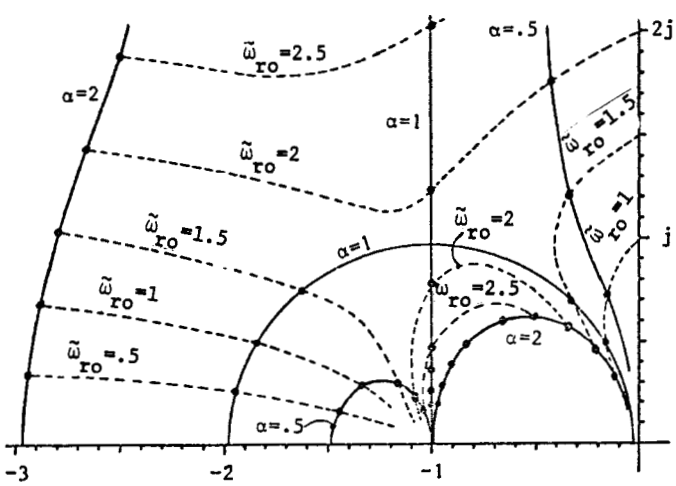

Fig. 2b. Low speed eigenvalues - rotor reference.

DYNAMIC RESPONSE WITH FINITE INERTIA

To illustrate the type of general results which can be obtained using the information in Table I, the poles of the overall transfer functions without external feedback will be examined. These poles are obtained from the roots (eigenvalues) of the characteristic equation of (24)

$$D\lambda + \tilde{K}\tilde{N}_r = 0 \qquad \tilde{K} = n\tilde{K}_r/J\alpha_r \tag{26}$$

and characterize the stability and dynamic response of an induction machine for small changes in input or load. A set of general root locii can be obtained and the non-dimensional loop gain $\tilde{K}$ provides a simple means of locating the operating point for a specific machine.

Root Locus End Points

For $\tilde{K} = 0$, the roots of (26) are the open loop poles given by (21) and Fig. 2 plus the inertial pole at the origin. At the other extreme as $\tilde{K}$ approaches infinity, the roots approach the zeros of $\tilde{G}_r$; given in terms of the polynomial for $\tilde{N}_r$ in Table I and illustrated for $\sigma = 0.08$ and $\tilde{\omega}_{so} = 0$ in Fig. 3. Note that for higher frequencies the complex pair of zeros "tracks" the high frequency open loop poles (compare Fig. 2a and Fig. 3). An excellent approximation for the zeros for high values of $\tilde{\omega}_o$ and small slip is

$$\lambda = -1 \ , \qquad -\tfrac{1}{2}\alpha(1+\sigma) \pm j\tilde{\omega}_o \tag{27}$$

The zeros are essentially independent of slip for normal operation since only $\tilde{\omega}_{so}^2$ occurs in the polynomial coefficients and $\tilde{\omega}_{so} \ll 1$ for typical machines. For high slip the real root moves toward the origin and crosses into the right half plane when the slip exceeds the slip for peak torque, yielding an unstable real root of (26) for operation beyond peak torque.

General Form of Root Locus

For normal operation (small slip) there are two basic types of root loci depending upon the non-dimensional stator frequency $\tilde{\omega}_o$ (and hence upon rotor speed $\tilde{\omega}_{ro}$). The two situations are illustrated in Fig. 4. For typical machines at nominal frequency, the operating point is on the lower, nearly vertical part of the high speed locus and the damping is quite acceptable. At very low stator frequencies the low speed locus applies and the damping can become very poor. If the non-dimensional gain $\tilde{K}$ is large enough, an actual instability can occur at some intermediate frequency when the high speed locus is still applicable.

The following sections develop a general quantitative root locus representation of these phenomena. Space limitations preclude treating all possible operating conditions and hence only the worst case of no load operation[7,8] is considered. Only the dominant roots are presented to conserve space, but it must be emphasized that the complete locus for all operating conditions could be treated by the same methods. In the following sections it is important to remember that $\tilde{\omega}_o$ and $\tilde{\omega}_{ro}$ are non-dimensional frequency and speed and that a particular machine may never operate on a "high frequency locus" if for example it has a very large value of α_r.

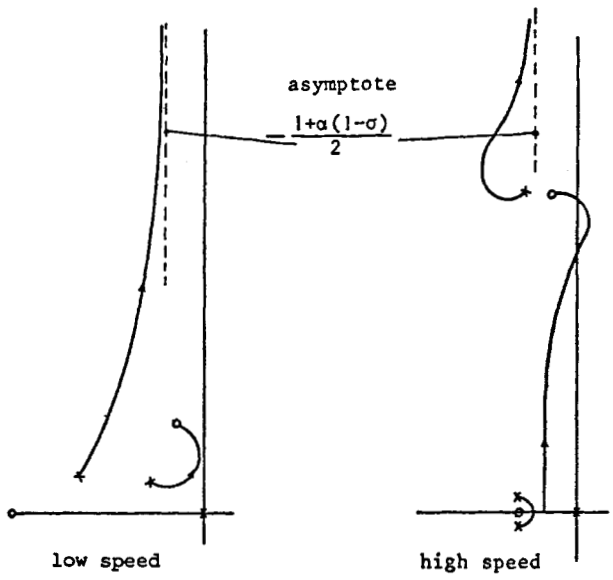

Fig. 4. General form of root locus for small slip.

High Frequency Operation ($\tilde{\omega}_o > 8$)

The simplest case occurs when $\tilde{\omega}_o$ is large since the high and low frequency poles and zeros are widely separated, good approximations for the pole and zero locations are available, and the real zero at -1 (see (27)) cancels one of the low frequency poles. The locus is illustrated in Fig. 5 for several values of α and symbolically for the general case. Clearly for low values of $\tilde{K}$ the high frequency poles and zeros cancel and the locus is well approximated as a second order system with poles at 0 and -1. A simple gain calibration formula then applies

$$\tilde{K}_b = \tilde{\omega}_b^2 + 1/4 \tag{28}$$

where $\tilde{K}_b$ and $\tilde{\omega}_b$ are the gain and frequency of a point on the locus as shown in Fig. 5.

For larger values of $\tilde{K}$ the high frequency pole and zero become significant and the locus bends into the right half plane. A small angle approximation (setting $\phi = \gamma$ in Fig. 5) yields a useful approximate expression for the zero damping frequency $\tilde{\omega}_c$

$$\tilde{\omega}_c = \tilde{\omega}_o/(1+\tfrac{1}{2}\alpha(1-\sigma)) \tag{29}$$

which in combination with (28) requires

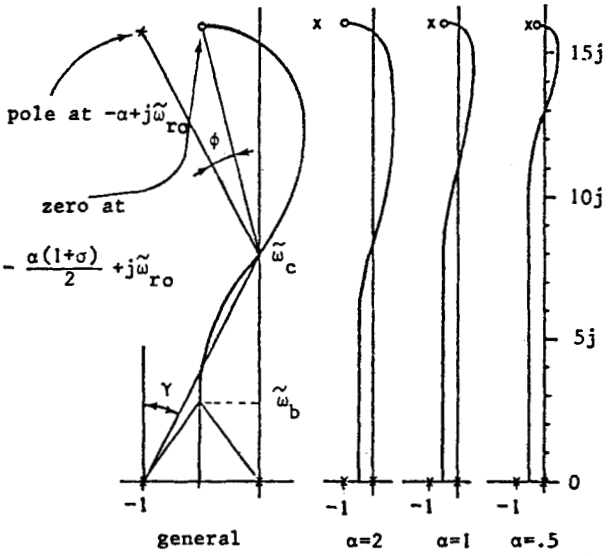

Fig. 5. High frequency root loci for zero slip ($\tilde{\omega}_o$=16).

$$\tilde{K} < \tilde{K}_c \approx \tilde{\omega}_c^2 = \tilde{\omega}_o^2/(1+\tfrac{1}{2}\alpha(1-\sigma)) \tag{30}$$

as an approximate stability criterion when the high frequency locus applies. At the other extreme when $\tilde{K}$ is small and the second order approximation is valid, (28) yields the result

$$\begin{aligned} \lambda &= -\tfrac{1}{2} \pm j\sqrt{\tilde{K}-\tfrac{1}{4}} && \tilde{K} \geq 1/4 \\ &= -\tfrac{1}{2} \pm \sqrt{\tfrac{1}{4}-\tilde{K}} && \tilde{K} \leq 1/4 \end{aligned} \tag{31}$$

for the dominant eigenvalues. This approximation holds until the frequency of the eigenvalue is of the order of one half of $\tilde{\omega}_c$ as can be seen from Fig. 5. Thus, for high frequency operation all the critical locus parameters can be expressed in equation form.

Intermediate and Low Frequency Operation

As the frequency is reduced the form of the locus gradually changes from the simple high frequency case to the closely packed pole zero pattern of the low frequency case. The transition region ($8 > \tilde{\omega}_o > 3$) is illustrated in Fig. 6a for $\sigma = 0.08$ and four values of α. The high frequency locus shape is retained down to about $\tilde{\omega}_o = 4$ except for large values of α. For these loci (29) is still a useful approximation; the error, however, increases as $\tilde{\omega}_o$ decreases and as α increases. The actual values of $\tilde{\omega}_c$ and $\tilde{K}_c$ can be read from Fig. 6a if σ is not significantly different from 0.08.

For low frequencies ($\tilde{\omega}_o < 3$) the unstable region disappears as shown in Fig. 6b. Furthermore the variation of

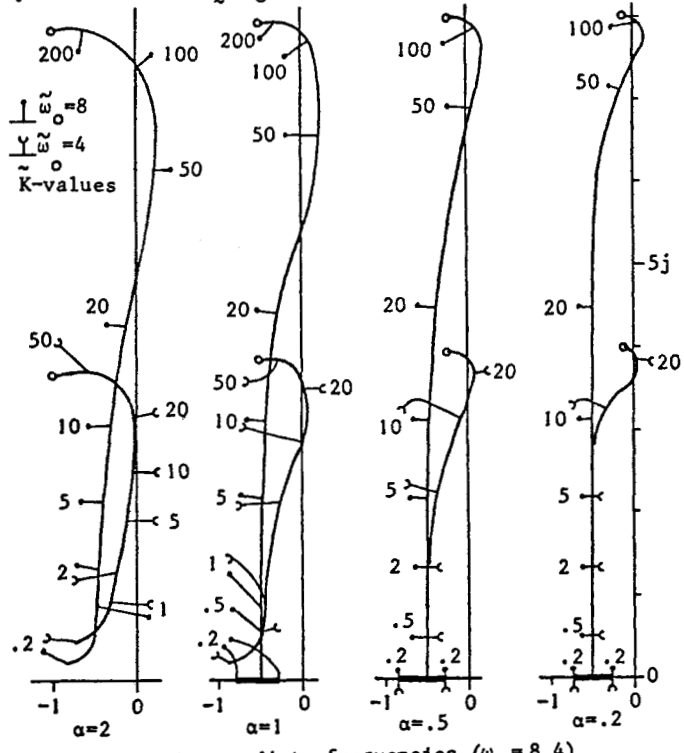

(a) Intermediate frequencies ($\omega_o = 8,4$)

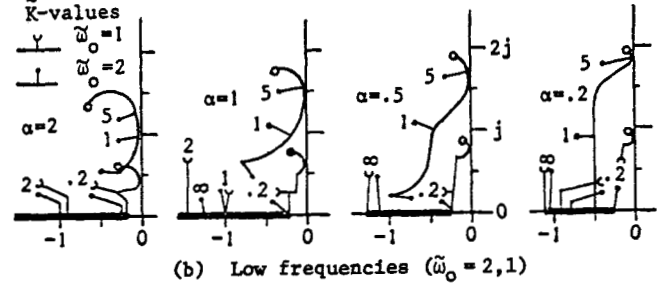

(b) Low frequencies ($\tilde{\omega}_o = 2,1$)

Fig. 6. Root loci for zero slip ($\sigma = 0.08$).

the roots with $\tilde{K}$ becomes very slow. Poor damping is possible and is associated with relatively low values of $\tilde{K}$. For these low frequency loci the value of σ becomes increasingly important with better damping associated with larger values of σ. The loci in Fig. 6 were obtained by computer analysis and additional loci or tables of minimum damping can be prepared to evaluate the influence of α, σ, and $\tilde{\omega}_o$ in more detail.

Non-Dimensional Gain

The utility of the generalized root loci of Figs. 5 and 6 is dependent on the simplicity of locating the operating point on the locus for a specific machine. This requires evaluation of the gain $\tilde{K}$ which is, fortunately, a simple computation. From (26) and Table I

$$\tilde{K} = n\, T_o/\omega_{so}\, J\alpha_r \qquad (32)$$

and the evaluation of $\tilde{K}$ hence requires only a steady state computation of the torque/slip-frequency ratio T_o/ω_{so}. Furthermore, because of the linearity of the torque speed curve near zero slip, this ratio is nearly a constant and need only be calculated once for a given machine (unless large slip operation is of interest). Note that except for very low frequencies where resistive effects are important, the value of $\tilde{K}$ is independent of frequency for operation at constant volts/hertz and can be easily corrected for changes in volts/hertz by multiplying by the square of the change. Perhaps the simplest means of finding $\tilde{K}$ for rated conditions is to use nameplate data to obtain rated torque and slip and evaluate $\tilde{K}$ as

$$\tilde{K} = n\, T_R/s_R\omega_{oR}\, J\alpha_r \qquad (33)$$

where T_R is rated torque, s_R is rated slip, and ω_{oR} is rated frequency. Clearly the effect of machine parameter changes on $\tilde{K}$ can be easily investigated by using steady state theory to find the effect of the parameter change on T_o/ω_{so}.

Typical Dynamic Performance

Computations for typical machines indicate $\tilde{K}$ ranges from values of the order of 0.1 for small or high inertia machines up to 10 or so for large machines. Because of these relatively low values of $\tilde{K}$ for typical machines, instability is quite unlikely except in very large machines. It is also apparent that the simple second order response associated with low gains on Figs. 5 and 6 is quite typical for most induction machines over a wide range of operating frequencies. However, because the gain is essentially independent of frequency, at some reduced frequency the damping of the dominant roots will reach minimum and then again increase for still smaller frequencies.

To illustrate these phenomena, consider a machine near the middle of the available size range (100 kW) with non-dimensional parameters $\alpha = 1$, $\sigma = 0.08$, $\alpha_r = 20$, $\tilde{K} = 3$. At nominal frequency (314 Hz) this machine has $\tilde{\omega}_o = 15.7$ and Fig. 5 with $\alpha = 1$ applies. The machine is well approximated as a second order system and (31) yields the dominant eigenvalues as $-\frac{1}{2} \pm j\ 1.66$ ($-10 \pm j\ 33.2$ sec^{-1}). As the frequency is reduced, maintaining constant volts/hertz, this situation remains essentially unchanged until a value of $\tilde{\omega}_o$ slightly larger than 4 is reached as shown on Fig. 6a. Below $\tilde{\omega}_o = 4$ the damping of the roots slowly decreases reaching a minimum near $\tilde{\omega}_o = 2$ (Fig. 6b) with an eigenfrequency of 1.40 (28.0 sec^{-1}). A further reduction in frequency increases the damping again although the change is not large (see $\tilde{\omega}_o = 1$ root locus on Fig. 6b).

The importance of the gain $\tilde{K}$ can easily be demonstrated by considering the effect on performance in this example if the value of $\tilde{K}$ is increased from 3 to 10. The initial performance at nominal frequency is similar except the eigenvalues have a higher frequency ($-\frac{1}{2} \pm j\ 3.12$ from (31)). This remains the case until about $\tilde{\omega}_o = 8$ at which point the damping begins to decrease reaching an unstable condition at $\tilde{\omega}_o = 4$ with an oscillation frequency of approximately 2.9 (58 sec^{-1}). Again for lower frequency the damping improves and the machine is stable with reasonable damping for $\tilde{\omega}_o = 2$.

Parameter Variations

A more complete set of generalized loci would permit very simple determination of the behavior of the roots for any machine in as much detail as desired. The loci given in Figs. 5 and 6 are already sufficient to allow general conclusions regarding the major effects of parameter variations on dynamics. Clearly high values of $\tilde{K}$ and low values of α_r tend to cause instability and poor damping. The effect of α is well illustrated in Fig. 6a where the effect is seen to depend strongly on $\tilde{\omega}_o$. The leakage parameter σ is relatively unimportant except at low frequencies where larger values of σ yield better damping.

To ascertain the influence of machine impedances it is only necessary to convert the impedance change to its effect on the non-dimensional parameters. Space limitations restrict the presentation to a few examples which illustrate the nature of the results which can be obtained:

1) an increase in the rotor resistance reduces $\tilde{K}$ as the square of the change, increases α_r linearly and decreases α. The result is better stability and a decrease in the normalized frequency at which minimum damping occurs (the real frequency may go up or down depending on the relative change in α_r).
2) an increase in the leakage inductance increases $\tilde{K}$ linearly and decreases α_r linearly. The result is a greater tendency toward instability but at a lower value of real frequency (since α_r is smaller).
3) a decrease in magnetizing reactance increases σ and improves the damping at reduced frequencies.
4) an increase in volts/hertz increases $\tilde{K}$ and results in a greater tendency toward instability and a larger value of the (normalized and real) frequency of minimum damping.

A more comprehensive study of dynamic response based on the methods developed in this paper is partially completed and will be presented in a subsequent paper.

CONCLUSION

The general results presented in this paper clearly demonstrate the value of complex variables in induction machine dynamic analysis. Of particular significance are: the decoupling resulting in excitation level dependent gain factors and general expressions for the zeros; the simple form and linear slip dependence of the open loop eigenvalues; the simplicity of form and guidance regarding relative significance of parameters resulting from introduction of non-dimensional parameters; and the general root loci and non-dimensional loop gain describing dynamic response without external feedback. These and other similar results depend strongly on the inherent symmetry of the machine and would be difficult to obtain using real variable methods.

APPENDIX A. TIME DOMAIN COMPLEX VARIABLE REPRESENTATION OF THE POLYPHASE INDUCTION MACHINE

Subject to the three phase to two phase power invariant transformation

$$\begin{bmatrix} v_a \\ v_b \\ v_c \end{bmatrix} = \sqrt{2/3} \begin{bmatrix} 1 & 0 & 1/\sqrt{2} \\ -1/2 & \sqrt{3}/2 & 1/\sqrt{2} \\ -1/2 & -\sqrt{3}/2 & 1/\sqrt{2} \end{bmatrix} \begin{bmatrix} v_{s\alpha} \\ v_{s\beta} \\ v_{so} \end{bmatrix}, \qquad (A\text{-}1)$$

$$\begin{bmatrix} v_{s\alpha} \\ v_{s\beta} \\ v_{so} \end{bmatrix} = \sqrt{2/3} \begin{bmatrix} 1 & -1/2 & -1/2 \\ 0 & \sqrt{3}/2 & -\sqrt{3}/2 \\ 1/\sqrt{2} & 1/\sqrt{2} & 1/\sqrt{2} \end{bmatrix} \begin{bmatrix} v_a \\ v_b \\ v_c \end{bmatrix} \quad \text{(A-2)}$$

the coupled circuit equations of the equivalent two phase machine in coil variables are[22]

$$[v_{s\alpha}, v_{s\beta}, v_{r\alpha}, v_{r\beta}]^T = \tilde{P}[i_{s\alpha}, i_{s\beta}, i_{r\alpha}, i_{r\beta}]^T \quad \text{(A-3)}$$

$$\tilde{P} = \begin{bmatrix} R_s + L_s p & 0 & Mp\cos\theta_r & -Mp\sin\theta_r \\ 0 & R_s + L_s p & Mp\sin\theta_r & Mp\cos\theta_r \\ Mp\cos\theta_r & Mp\sin\theta_r & R_r + L_r p & 0 \\ -Mp\sin\theta_r & Mp\cos\theta_r & 0 & R_r + L_r p \end{bmatrix}$$

$$T = nM[(i_{s\beta}i_{r\alpha} - i_{s\alpha}i_{r\beta})\cos\theta_r - (i_{s\alpha}i_{r\alpha} + i_{s\beta}i_{r\beta})\sin\theta_r] \quad \text{(A-4)}$$

where the reference polarities and variables are defined in Fig. A-1. The zero sequence equations are omitted from (A-3) based on the assumption the machine has no neutral connection.

To obtain time domain complex equations, define the complex variables

$$\bar{v}_{sc} = v_{s\alpha} + jv_{s\beta} \qquad \bar{i}_{sc} = i_{s\alpha} + ji_{s\beta}$$
$$\bar{v}_{rc} = v_{r\alpha} + jv_{r\beta} \qquad \bar{i}_{rc} = i_{r\alpha} + ji_{r\beta} \quad \text{(A-5)}$$

and apply these definitions to (A-3) and (A-4) to produce the coil variable complex equations

$$\bar{v}_{sc} = (R_s + L_s p)\bar{i}_{sc} + Mp(\varepsilon^{j\theta_r}\bar{i}_{rc})$$
$$\bar{v}_{rc} = Mp(\varepsilon^{-j\theta_r}\bar{i}_{sc}) + (R_r + L_r p)\bar{i}_{rc} \quad \text{(A-6)}$$

$$T = nM\, iM[\bar{i}_{sc}(\varepsilon^{j\theta_r}\bar{i}_{rc})^*] \quad \text{(A-7)}$$

in which the complex exponential function $\varepsilon^{j\theta r}$ compactly represents all of the trigonometric functions in (A-3) and (A-4). Similarly, the transformation equations of (A-1) and (A-2) become

$$\bar{v}_{sc} = \sqrt{2/3}\,(v_a + \bar{a}v_b + \bar{a}^2 v_c) \quad \text{(A-8)}$$

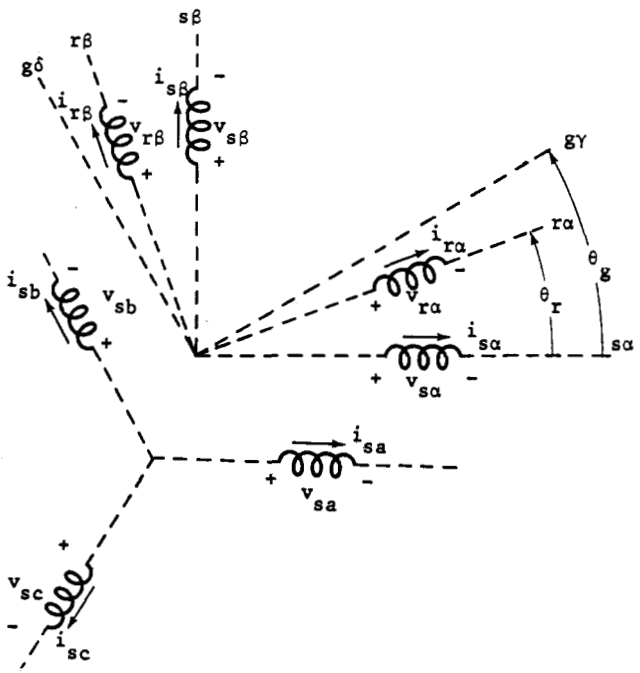

Fig. A-1. Coil and axis configuration and reference polarity two phase and three phase machines.

$$v_a = \sqrt{2/3}\,\mathrm{Re}[\bar{v}_{sc}] \quad , \quad v_b = \sqrt{2/3}\,\mathrm{Re}[\bar{a}^2\bar{v}_{sc}]$$
$$v_c = \sqrt{2/3}\,\mathrm{Re}[\bar{a}\,\bar{v}_{sc}] \quad \text{(A-9)}$$

where $\bar{a}$ is the complex quantity $\varepsilon^{j2\pi/3}$.

The transformation of the coil variable complex equations to stator or synchronously referred variables is readily accomplished by defining general (rotating reference) variables as follows

$$\bar{i}_{sg} = \varepsilon^{-j\theta g}\bar{i}_{sc} \qquad \bar{i}_{rg} = \varepsilon^{-j(\theta_g - \theta_r)}\bar{i}_{rc}$$
$$\bar{v}_{sg} = \varepsilon^{-j\theta g}\bar{v}_{sc} \qquad \bar{v}_{rg} = \varepsilon^{-j(\theta_g - \theta_r)}\bar{v}_{rc} \quad \text{(A-10)}$$

where θ_g is a general reference angle locating the rotating reference axes of the new variables as shown in Fig. A-1. Introducing these variables into the coil variable equations, carrying out the differentiation, and cancelling the resulting common exponential factors produces the general transformed equations.

$$\bar{v}_{sg} = [R_s + L_s(p+j\omega_g)]\bar{i}_{sg} + M(p+j\omega_g)\bar{i}_{rg} \quad \text{(A-11)}$$
$$\bar{v}_{rg} = M(p+j(\omega_g - \omega_r))\bar{i}_{sg} + [(R_r + L_r(p+j(\omega_g - \omega_r))]\bar{i}_{rg}$$

$$T = nM\,\mathrm{Im}[\bar{i}_{sg}\,\bar{i}^*_{rg}] \quad \text{(A-12)}$$

where $\omega_g = p\theta_g$ is the speed of the reference system. These equations are the complex variable form of the equations resulting from the rotating coordinate transformations of real variable theory (arbitrary reference frames[4]). The complex operator p+jω is a very compact representation of the existence of both speed and transformer voltages in the machine.

It is convenient to define complex operational impedances and write (A-11) as

$$\bar{v}_{sg} = \bar{Z}_{sg}\bar{I}_{sg} + \bar{Z}_{mg}\bar{I}_{rg}$$
$$\bar{v}_{rg} = \bar{Z}_{dg}\bar{I}_{sg} + \bar{Z}_{rg}\bar{I}_{rg} \quad \text{(A-13)}$$

where the definitions of the impedances are apparent by comparison of (A-11) and A-13). The instantaneous electrical frequencies which appear in the various impedances depend upon the choice of the reference system. The important systems and the corresponding complex operational impedances and complex voltage associated with balanced sinusoidal excitation are:

Stator reference: ($\omega_g = 0$) (A-14)

$$\bar{Z}_{ss} = R_s + L_s p \qquad \bar{Z}_{ms} = Mp$$
$$\bar{Z}_{ds} = M(p - j\omega_r) \qquad \bar{Z}_{rs} = R_r + L_r(p - j\omega_r)$$
$$\bar{v}_{ss} = \sqrt{3}\,V_{rms}\,\varepsilon^{j(\omega t + \phi)}$$

Rotor reference: ($\omega_g = \omega_r$) (A-15)

$$\bar{Z}_{sr} = R_s + L_s(p + j\omega_r) \qquad \bar{Z}_{mr} = M(p + j\omega_r)$$
$$\bar{Z}_{dr} = Mp \qquad \bar{Z}_{rr} = R_r + L_r p$$
$$\bar{v}_{sr} = \sqrt{3}\,V_{rms}\,\varepsilon^{j((\omega - \omega_r)t + \phi - \phi_g)}$$

Synchronous reference: ($\omega_g = \omega$) (A-16)

$$\bar{Z}_{s\omega} = R_s + L_s(p + j\omega) \qquad \bar{Z}_{m\omega} = M(p + j\omega)$$
$$\bar{Z}_{d\omega} = M(p + j\omega_s) \qquad \bar{Z}_{r\omega} = R_r + L_r(p + j\omega_s)$$
$$v_{s\omega} = \sqrt{3}\,V_{rms}\,\varepsilon^{j(\phi - \phi_g)}$$

APPENDIX B — LINEARIZED EQUATIONS OF THE POLYPHASE INDUCTION MACHINE USING TIME DOMAIN COMPLEX VARIABLES

Allowing all variables in (A-12) and (A-13) to have a small signal component (perturbation) added to the steady state solution such that each variable has the form $\bar{x} = X_o + \Delta\bar{x}$ results in the following expanded form of the synchronous referred complex variable equations

$$\bar{v}_{so} + \Delta\bar{v}_s = [R_s + L_s(p+j\omega_o+j\Delta\omega)](\bar{I}_{so}+\Delta\bar{I}_s) + M(p+j\omega_o+j\Delta\omega)(\bar{I}_{ro}+\Delta\bar{I}_r) \quad (B\text{-}1)$$

$$0 = M(p+j\omega_{so}+j\Delta\omega_s)(\bar{I}_{so}+\Delta\bar{I}_s) + [R_r+L_r(p+j\omega_{so}+j\Delta\omega_s)](\bar{I}_{ro}+\Delta\bar{I}_r)$$

$$T_o + \Delta T = nM[(\bar{I}_{so}+\Delta\bar{I}_s)(\bar{I}_{ro}+\Delta\bar{I}_r)^*] = \frac{J}{n}p(\omega_{ro}+\Delta\omega_r) + T_{L0} + \Delta T_{L0} \quad (B\text{-}2)$$

Since $\bar{v}_{so}$ is constant in a synchronous reference, the steady state solution is also a set of complex constants. A set of relations defining the steady state solution can be obtained from (B-1) and (B-2) by dropping all derivative terms and incremental variables and setting the frequencies equal to their steady state values.

$$\bar{v}_{so} = (R_s + j\omega_o L_s)\bar{I}_{so} + j\omega_o M\bar{I}_{ro} = \bar{Z}_{so}\bar{I}_{so} + \bar{Z}_{mo}\bar{I}_{ro} \quad (B\text{-}3)$$

$$0 = j\omega_{so}M\bar{I}_{so} + (R_r + j\omega_{so}L_r)\bar{I}_{ro} = \bar{Z}_{do}\bar{I}_{so} + \bar{Z}_{ro}\bar{I}_{ro}$$

$$T_o = nM\,\mathrm{Im}[\bar{I}_{so}\,\bar{I}^*_{ro}] = T_{Lo} \quad (B\text{-}4)$$

Carrying out the linearization by neglecting products of small signal (Δ) variables and subtracting the steady state solution of (B-3) and (B-4) yields the linearized equations relating the small signal variables

$$\Delta\bar{v}_s = \bar{Z}_s\Delta\bar{I}_s + \bar{Z}_m\Delta\bar{I}_r + \bar{\phi}_{so}\Delta\omega \quad (B\text{-}5)$$

$$0 = \bar{Z}_d\Delta\bar{I}_s + \bar{Z}_r\Delta\bar{I}_r + \bar{\phi}_{ro}\Delta\omega_s$$

$$T = nM\,\mathrm{Im}[\bar{I}_{so}\Delta\bar{I}^*_r + \bar{I}^*_{ro}\Delta\bar{I}_s] = \frac{J}{n}p\Delta\omega_r + \Delta T_L \quad (B\text{-}6)$$

where

$$\bar{Z}_s = R_s + L_s(p+j\omega_o) \qquad \bar{Z}_m = M(p+j\omega_o)$$
$$\bar{Z}_d = M(p+j\omega_{so}) \qquad \bar{Z}_r = R_r + L_r(p+j\omega_{so}) \quad (B\text{-}7)$$
$$\bar{\phi}_{so} = j(L_s\bar{I}_{so} + M\bar{I}_{ro}) \qquad \bar{\phi}_{ro} = j(M\bar{I}_{so} + L_r\bar{I}_{ro})$$

NOTATION

Specific symbols are defined where introduced in the text. The following general symbols are used throughout.

$\bar{x}$	complex quantity	ω	stator frequency
$\bar{x}^*$	conjugate of $\bar{x}$	ω_s	slip frequency
$\mathrm{Re}[\bar{x}]$	real part of $\bar{x}$	ω_r	rotor frequency
$\mathrm{Im}[\bar{x}]$	j-part of $\bar{x}$	V_{rms}	line-neutral rms voltage
$\tilde{x}$	normalized quantity	σ	$1 - M^2/L_sL_r$
x_o	steady state quantity	n	pole pairs
Δx	incremental quantity	p	time derivative
		j	complex operator

ACKNOWLEDGMENT

The research reported in this paper was carried out while D. W. Novotny was on leave at the University of Technology Eindhoven, Netherlands. Research salary support from the University of Technology Eindhoven and from the Research Committee of the University of Wisconsin - Madison is gratefully acknowledged.

REFERENCES

1. R. G. Schieman, E. A. Wilkes, H. E. Jordan, "Solid State Control of Electric Drives", Proc. IEEE 62, No. 12, pp. 1643-1660, 1974.
2. H. E. Jordan, "Analysis of Induction Machines in Dynamic Systems", IEEE Trans. PAS-84, No. 11, pp. 1080-1088, 1965.
3. H. E. Jordan, "Digital Computer Analysis of Induction Machines in Dynamic Systems", IEEE Trans. PAS-86, No. 6, pp. 722-728, 1967.
4. P. C. Krause, C. H. Thomas, "Simulation of Symmetrical Induction Machinery", IEEE Trans. PAS-84, No. 11, pp. 1038-1053, 1965.
5. P. J. Lawrenson, J. M. Stephenson, "Note on Induction Machine Performance with a Variable Frequency Supply", Proc. IEE 113, No. 10, pp. 1617-1623, 1966.
6. B. V. Jayawant, K. N. Bateson, "Dynamic Performance of Induction Motors in Control Systems", Proc. IEE 115, No. 12, pp. 1865-1870, 1968.
7. G. J. Rogers, "Linearized Analysis of Induction Motor Transients", Proc. IEE 112, No. 10, pp. 1917-1925, 1965.
8. R. H. Nelson, T. A. Lipo, P. C. Krause, "Stability Analysis of a Symmetrical Induction Machine", IEEE Trans. PAS-88, No. 11, pp. 1710-1717, 1969.
9. T. A. Lipo, A. B. Plunkett, "A Novel Approach to Induction Motor Transfer Functions", IEEE-IAS Annual Meeting Conference Record, pp. 441-449, 1973.
10. J. J. Cathey, R. K. Calvin, A. K. Ayoub, "Transient Load Model of an Induction Motor", IEEE Trans. PAS-92, No. 4, pp. 1399-1406, Jul/Aug 1973.
11. J. T. Salihi, "Simulation of Controlled Slip Variable Speed Induction Motor Drive Systems", IEEE Trans. IGA-5, No. 2, pp. 149-157, 1969.
12. P. Bowler, B. Nir, "Steady State Stability Criterion for Induction Motors", Proc. IEE 121, No. 7, pp. 663-667, 1974.
13. Y. H. Ku, "Transient Analysis of Rotating Machines & Stationary Networks by Means of Rotating Reference Frames", AIEE Trans., Pt. 1 70, pp. 943-957, 1951.
14. W. V. Lyon, "Transient Analysis of Alternating Current Machinery", (book) The Technology Press of M.I.T and John Wiley & Sons Inc., New York, 1954.
15. K. P. Kovacs, "Symmetrical Components in Polyphase Machines", (book in German), Druck von W. Rosch and Co., Bern, 1962.
16. T. J. Takeuchi, "Theory of SCR Circuits and Application to Motor Control", (book) Tokyo Electrical Engineering College Press, 1968.
17. I. Racz, "Dynamic Behavior of Inverter Controlled Induction Motors", Proc. 3rd Congress of IFAC, Vol. I, pp. 4B1-4B7, June 1965.
18. E. M. Sabbagh, W. Sherman, "Characteristics of an Adjustable Speed Polyphase Induction Machine", IEEE Trans. PAS-87, No. 3, pp. 613-624, 1968.
19. J. G. Szablya, J. M. Bressane, "Transfer Functions of AC Machines", IEEE Trans. PAS-92, No. 1, pp. 177-186, 1973.
20. D. W. Novotny, "Switching Function Representation of Polyphase Inverters", IEEE-IAS Annual Meeting Conference Record, 1975.
21. D. W. Novotny, "Steady State Performance of Inverter Driven Induction Machines by Means of Time Domain Complex Variables", IEEE Winter Power Meeting, 1975.
22. C. V. Jones, "The Unified Theory of Electrical Machines" (book), Butterworths, London, 1967.

Discussion

V. R. Stefanovic (Concordia University, Montreal, Canada): The authors are to be complimented for developing a new analytical procedure for the calculation of induction motor transfer functions. The transfer function approach is receiving renewed attention (9, 23) after some of the disadvantages of other methods in the system transient analysis and design have been recognized (24). It is expected that this trend will continue, especially in the treatment of motor drives, where the number of inputs and outputs is relatively small. By using complex time variables, the authors have provided not only a new tool for the analysis, but were also able to significantly simplify the complex problem of induction motor transients.

The authors have made a wise choice by giving special attention to the speed-torque transfer function which may be regarded as the motor equivalent output impedance. As such, it is one of the most important drive transfer functions and describes fully the induction motor dynamic characteristics regardless of the input voltage-frequency relationship.

Would the authors comment on the following points:

1. The method presented here is restricted to induction motors operating without any current feedbacks. A much more general method (named Direct Method) has been proposed recently (23). Within standard linearity constraints this method permits to predict the speed-torque transfer function of any electric drive, operating with any number of feedback loops and having an arbitrary controller configuration. In addition to this, the method is simple and comes out directly from the drive equations in the synchronous reference frame. Since both complex time variable and Direct Method are based on the symmetry of electrical machines, I feel that some of the restrictions in the method presented here may be removed so that it can be extended to other types of motor drives.

2. The authors have provided us with a very useful and simple formula for the analytical computation of the transfer function zeros – equations [13], [16] and [21]. (The poles of G_r become the zeros of the overall speed – load torque transfer function). The remaining part of the paper deals then almost exclusively with the transfer function poles – equation [26]. The zeros, however, play a very important role. For example, it was found that for a motor without external feedbacks which operates above 10-15 hz. the four poles determined by the motor electrical system are effectively cancelled by four zeros (23). This then leaves a first order speed-torque transfer function with a pole determined by a slope of the motor torque – speed curve, total drive inertia and friction. It should be possible to obtain the same result by the complex time variable method.

3. The statement which follows equation [25] appears to be unclear. When a feedback loop is closed, this is done usually through a PI controller, which very often includes some compensating network. Consequently, the number of poles and zeros in the closed loop transfer function is increased by the order of the added drive controller. Even if the statement refers to a controller with a proportional gain only, so that the number of poles and zeros is unchanged, the transfer function gain will change. (Consider for example a drive which in addition to the frequency loop has a feedback loop controlling the motor voltage or current. Without such a loop any drive with constant slip speed becomes unstable).

4. The statement that the gain K, defined by the equation [32] is essentially independent of the input frequency is somewhat dubious. This gain is proportional to the slope of the motor torque-speed curve. Generally, this slope starts to decrease as the input frequency is lowered reducing the motor damping (25). Our measurements on a typical 5 hp motor showed for example that this decrease starts when the frequency is lowered below 20 hz and becomes very pronounced below 10 hz. If such a motor operates in a standard range of up to 60 hz, the gain would not be constant over 16% (or 30%) of the motor speed range.

5. Equations [2], [5] and figure (1) indicate that the drive total friction is neglected. This tends to give slightly pessimistic stability results. (Closure of (25)). There is no apparent reason why the method, as presented here could not include the total drive friction. (Note that lumping the friction together with the load torque is not dynamically equivalent to treating it as a part of the mechanical system, figure 1b).

REFERENCES

(23) V. R. Stefanovic and T. H. Barton: "The Speed Torque Transfer Function of Electric Motor Drives", IEEE-IAS Annual Meeting Conference Record, pp. 359-368, 1975.

(24) I. M. Hofowitz and U. Shaked: "Superiority of Transfer Function over State Variable Methods in Linear Time-Invariant Feedback System Design", IEEE Trans. on Automatic Control, Vol. AC-20, February 1975, pp. 84-97.

(25) R. H. Nelson, T. A. Lipo and P. C. Krause: "Stability Analysis of a Symmetrical Induction Machine", IEEE Trans. on Power Apparatus and Systems", Vol. PAS-88, No. 11, November 1969.

Manuscript received February 12, 1976.

D. W. Novotny and **J. H. Wouterse**: The authors thank Mr. Stefanovic for his remarks regarding the analytical approach of the paper and welcome the opportunity to comment on the specific points raised in the discussion. The clarification of these points plus the two additional references (the third added reference [25] is already given as reference 8 in the paper) relating to the value of transfer functions and to a new alternative approach are valuable additions to the paper.

Regarding the specific numbered items in the discussion:

1. The "Direct Method" presented by Mr. Stefanovic in reference 23 is a method which yields the speed-torque transfer function of a drive system in terms of the solution of two separate eigenvalue problems. In general this method requires numerical solution for the two sets of eigenvalues. In comparison, the method of the paper yields a partly closed form solution to a more restricted problem. The authors share the discusser's feeling that some of the present restrictions on the method of the paper can be removed. However, it is unlikely that the general applicability of the "Direct Method" can be attained since the type of symmetry required for effective use of complex variables does not appear to exist except in induction machines. The complex variable method offers the advantage of providing very general closed form solutions for induction machines including speed-voltage and speed-frequency transfer functions in addition to the speed-torque transfer function. Thus the two methods offer different types of generality; the "Direct Method" in the sense of application to a wide variety of drives and complex variables in the sense of a wide variety of conditions in induction motor drives.

2. Although not specifically identified in the paper, the cancellation of the speed-torque transfer function ($\Delta\omega_r/\Delta T_L$ in Fig. 1b) zeros with four of the poles can be seen in Fig. 6. When the non-dimensional gain $\tilde{K}$ is small, the roots (poles) on the loci of Fig. 6 are close to their starting points. However, these starting points, except for the one at the origin, are the zeros of the speed-torque transfer function and hence cancellation occurs.

This result can be made quantitative by using equation 31

$$\lambda = -\tfrac{1}{2} \pm \sqrt{\tfrac{1}{4} - \tilde{K}} \qquad \tilde{K} \leq \tfrac{1}{4}$$

which is valid when the normalized frequency $\tilde{\omega}_o$ is sufficiently large (see text below equation 31). If $\tilde{K}$ is small compared to ¼, the two roots can be obtained from a binomial expansion as

$$\lambda = -\tilde{K} \quad \text{and} \quad -1 + \tilde{K}$$

The smaller root at $-\tilde{K}$ is the only pole which is not cancelled by a zero. Using the definition of $\tilde{K}$ in equation 32, the (dimensional) value of this root is

$$\lambda\alpha_r = nT_o/\omega_{so}J$$

which is in agreement with the qualitative result given in the discussion. Note, however, that in addition to requiring a sufficiently high frequency, a critical criterion of whether this first order approximation is valid is that $\tilde{K} \ll \tfrac{1}{4}$. Thus, since $\tilde{K}$ increases as the size of the machine increases, large machines will not be adequately represented as a first order system even at nominal frequency.

3. The statement following equation 25 refers only to the use of a unit gain loop to hold constant slip. For this case the statement in question is correct. The authors agree that such a loop alone results in a constant torque drive and must have a second loop controlling voltage or current to be practical. Knowledge of the transfer function of the machine with the slip control loop is useful in the design of this second control loop.

4. The non-dimensional gain $\tilde{K}$ does indeed decrease as the input frequency decreases (at constant volts/hertz) as a result of the decreased slope of the speed-torque curve. This change is caused by the presence of stator resistance and becomes appreciable when the resistance is no longer small compared to the reactances of the machine. The frequency at which this occurs depends essentially on the values of α and α_r. However, α is normally close to unity and hence the critical parameter is α_r, which is strongly dependent on machine size. Thus, in general, large machines with small values of α_r can be run to quite low frequencies before $\tilde{K}$ decreases significantly. Small machines with large values of α_r will show the effect much more rapidly.

The influence of this change in $\tilde{K}$ is to alter the point of operation on the locus diagrams of Fig. 6. In general, a reduction in $\tilde{K}$ would tend to produce better damping as can be seen by examining the figure. The

Manuscript received April 12, 1976.

generally poorer damping associated with low frequency operation is therefore not caused by the reduced value of $\tilde{K}$, but by the motion of the poles and zeros resulting from the frequency change itself.

5. Drive system friction can be included by replacing the inertial integration in Fig. 1b by the appropriate time constant. This has the effect of moving the origin pole in Figs. 4, 5 and 6 slightly to the left of the origin. Note that this will have only a small effect if $\tilde{K}$ and $\tilde{\omega}_o$ are large but will move the dominant real pole leftward for small values of $\tilde{K}$ (when pole-zero cancellation occurs). As in item (2), the important role of $\tilde{K}$ as a general indicator of the dynamics of an induction machine and of the influence of various parameter changes is evident.

The authors would also like to correct a symbolic error in the paper. The symbol $\tilde{D}$ in equation 18 represents the real variable normalized denominator of the transfer functions and contains two pairs of complex conjugate poles. Unfortunately, the same symbol was used in the complex variable expressions of equations 19 and 20 where only two of these poles are represented. The two poles given by equation 20 must be augmented by their complex conjugates to give $\tilde{D}$ in equation 18. This is best handled by replacing $\tilde{D}$ in equations 19 and 20 by a new symbol $\tilde{F}$ and defining $\tilde{D}$ in equation 18 as $\tilde{D} = \tilde{F}\,\tilde{F}^*$.